

Characterization of Spin Coated Tin Oxide Thin Films for Optoelectronic Applications

M. Maache^{1,2,*}, A. Chala^{2,3}, T. Devers⁴

¹ Department of Physics, Ziane Achour University, 17000 Djelfa, Algeria

² PLTFA, Physical Laboratory of Thin Films and Applications, Mohamed Khider University, 07000 Biskra, Algeria

³ Department of Science of Matter, Mohamed Khider University, 07000 Biskra, Algeria

⁴ University of Orléans, ICMN-UMR 7374 CNRS, IUT of Chartres, 28000 Chartres, France

(Received 25 May 2019; revised manuscript received 15 June 2020; published online 25 June 2020)

Sol-gel technique was operated to obtain pure tin oxide (SnO₂) thin films. The films were grown at room temperature on clean glass substrates by a spin coating method. Tin (II) chloride dehydrate was used as a starting material, and 2-propanol was used as the solvent. Tin molarity was kept [Sn²⁺] = 0.3 M. The SEM micrographs of the elaborated films show that they are composed of very fine-grained microstructure of SnO₂. XRD analysis reveals that all annealed films consist of single phase SnO₂, the diffractograms indicate the presence of (100), (101), (211) peaks corresponding to the tetragonal phase without any secondary phases. The scanning electron microscopy and the atomic force microscopy images show the evolution of the different surface morphologies; all films have homogeneous and uniform surface morphology. The transmission electron microscopy measurements confirm that the prepared films are nanocrystalline. Furthermore, the influence of multiple coating on the optoelectronic properties of SnO₂ thin films is examined. In the visible region, the transmittance is greater than 85 %. The resistivity of SnO₂ thin films decreases significantly with the thickness. The estimated maximum value of conductivity is 2.72 (Ω.cm)⁻¹.

Keywords: SnO₂, Sol-gel, Spin coating, Conductivity, Optoelectronic.

DOI: [10.21272/jnep.12\(3\).03010](https://doi.org/10.21272/jnep.12(3).03010)

PACS number: 68.00.00

1. INTRODUCTION

Transparent conducting films have received considerable attention of the researchers owing to their useful properties such as photoluminescence, electroluminescence, or nonlinear optical properties, which may lead to new optoelectronic devices with greater performance [1].

In particular, we are interested in the study of tin dioxide (SnO₂) based films as a TCO metal oxide [2], most important because of their excellent optical, electrical, and gas sensing properties [3]. It is a direct *n*-type wide band gap semiconductor of about 3.87-4.3 eV [2, 4], which has been extensively used in various technological applications such as gas sensors [5, 6], heat reflectors, flat display devices, photovoltaic cells, and thin film transistors [7].

Plethora techniques have been experienced to obtain SnO₂ thin films. These include radio frequency (RF) magnetron sputtering [8], evaporation [9], chemical vapor deposition CVD [10], spray pyrolysis [11] and sol-gel processes [12, 13]. Among these techniques, the sol-gel is non-vacuum, wet and chemical method. It offers the greatest possibility of preparing a film with large area at low cost for technological applications.

Spin coating was selected to synthesize nanostructured SnO₂ thin films. We chose this method because it is quiet and has the merits of simplicity and the flexibility for process modifications, and it has advantages of excellent compositional control, uniformity of the film thickness and lower crystallization temperature.

However, in thin film form, depending on the deposition technique its structure can be polycrystalline or amorphous [14]. There are many factors affecting the crystallization behavior of SnO₂ thin films, such as the

annealing temperature, the molar ratio of the starting material and the thickness.

The present study investigated the characteristics of SnO₂ thin films prepared by the spin-coating process. The structural, electrical and optical properties were examined in relationship with the variation in thickness, as well as obtaining uniform films of a quality necessary for optoelectronic applications.

2. EXPERIMENTAL

Using SPIN 150 system, we have grown pure SnO₂ thin films on glass substrates. Solutions of compound precursors were prepared. Tin chloride dehydrate (SnCl₂·2H₂O) was used as a starting material. It was dissolved in 2-propanol [(CH₃)₂CHOH], and the concentration of tin was kept 0.3 mol/l. After continuous magnetic stirring for 1 h, a transparent homogeneous and stable sol was obtained. The spin coating was made one day after the sol preparation.

The coating solution of approximately 0.2 ml was dropped and spin-coated with 3000 rpm for 35 s (the spinner reached 3000 rpm after 5 s which was maintained for 25 s). For each layer, the films were followed by drying in air at 250 °C for 5 min in a furnace to evaporate the solvent and remove organic residuals and impurities in the coated films. To investigate the effect of multiple coating, the above procedure (spinning + drying = cycle) was repeated 1-5 times. Then, the films were annealed into furnace at 450 °C for 1 h. This heat treatment decomposed the precursor film and oxidized it so as to produce SnO₂ film. The choice of these parameters was justified from preliminary investigation. Fig. 1 shows the flow diagram for SnO₂ films pre-

* moumos2001@gmail.com

pared by sol-gel spin-coating process, a similar process as described in our previous work [15].

Finally, the multilayered SnO₂ films were left to cool down at room temperature and they were ready for measurements.

The thicknesses of SnO₂ thin films were measured using a Dektak 150 surface profiler. They were characterized by using a variety of techniques. For surface topology and to confirm the presence of fine particles, a scanning electron microscope (SEM), a LEO 1430 VP microscope and an atomic force microscope (AFM: digital Instrument NanoScope (R) III, Veeco Digital Instruments Version 5.30r2) were used. The structural properties of the films were determined by X-ray diffractometer using CuK_α radiation (wavelength $\lambda = 1.54056 \text{ \AA}$) with a Philips X-ray diffractometer (X'pert PRO, MPD PANalytical) operated at 40 kV, 20 mA. The transmission electron microscopy (TEM) was undertaken with a Philips CM20 (at an acceleration voltage of 200 kV). The optical transmission spectra for SnO₂ films of different thicknesses were obtained by a double-beam spectrophotometer (JASKO V-530, UV-VIS Version: 1.53) at room temperature. Finally, the electrical conductivity of thin films was measured using four-point probe method.

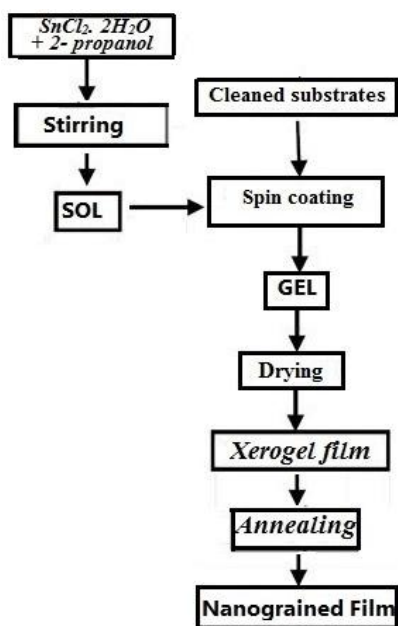


Fig. 1 – Flow diagram of spin coating process to elaborate SnO₂ thin films

3. RESULTS AND DISCUSSION

3.1 Thickness

The thickness increases normally with the number of layers. As can be seen from Fig. 2, a linear increase in the thickness of the samples with increasing the cycle number is accompanied by an increase in the material volume operated in the plane and in the thickness.

3.2 Film Structure and Morphology

The surfaces observed of SnO₂ thin films are homogeneous, and they have very good adhesion to the sub-

strate. Fig. 3 shows a SEM picture of the pure SnO₂ film prepared by spin coating. It indicates that the films have a very compact microstructure, and the crystal grains cannot be observed.

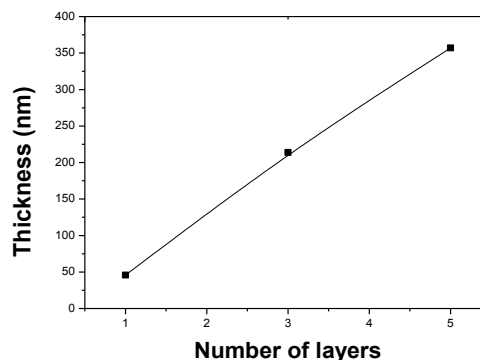


Fig. 2 – Variation of the SnO₂ thin film thickness versus the number of layers

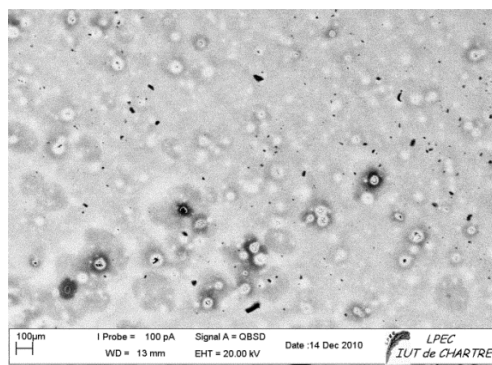


Fig. 3 – SEM photograph of SnO₂ thin film of 5 cycles, spin coated from $M = 0.3$ of starting solution on a glass substrate, and annealed at 450 °C for 1 h in air

As shown in Fig. 3 and Fig. 4, larger grains have germinated of size about 20-100 μm on the film mat, they come from the precursor elements that have not reached the hydrolysis reaction. An X-ray microanalysis profile was made with SEM to verify the elements corresponding to films. Fig. 4 shows a general aspect of these analyses. Two places are distinguished in the figure, where the first, indicated (1), corresponds to the white spots and the second, denoted (2), corresponds to the gray mat, the presence of tin and oxygen is clearly detected. The presence of chlorine from the precursors indicates incomplete dissolution; the elements silicon, sodium and calcium are detected because of the substrate.

X-ray diffraction (XRD) was carried out on all the samples with different thicknesses to determine the structure of the films. The diffraction patterns (Fig. 5) of pure SnO₂ films show that all observed peaks can be indexed to the known tetragonal (rutile) phase without any secondary phase. No diffraction peaks from other species or from parasitic phase can be detected. The characteristic peaks are consistent with those reported in the literature [16].

The intensities of the peaks increase with the increase in the number of cycles, as the amount of material increases, therefore the film thickness increases, which intensifies the diffraction peaks and improves the crystallinity of the material.

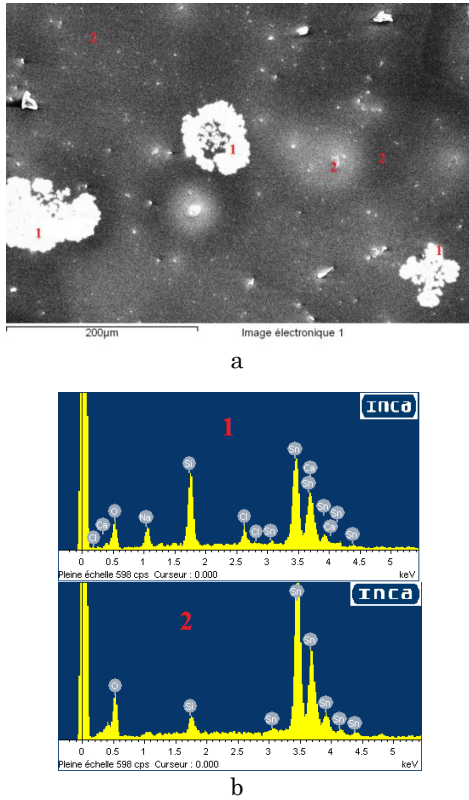


Fig. 4 – SEM micrographs (a) and X-ray microanalysis profiles (b): two locations (1) and corresponding to SnO₂ (2)

The lattice constants $a = b$ and c of SnO₂ films were calculated using the analytical method, where the distance d_{hkl} is governed by the well-known analytical law [17]:

$$\frac{1}{d_{hkl}^2} = \frac{h^2 + k^2}{a^2} + \frac{l^2}{c^2}. \quad (3.1)$$

The calculated d_{hkl} values are in good agreement with standard ones (ICDD pdf No. 00-001-0625). The lattice parameters were found to be $a = b = 0.477$ nm and $c = 0.3177$ nm. We may conclude that the films have a good structural quality.

According to the full width at half-maximum (FWHM) of the diffraction peaks, the mean size of SnO₂ nanoparticles D_{hkl} was calculated using Scherrer's formula:

$$D_{hkl} = \frac{k\lambda}{B_{hkl} \cos \theta_{hkl}}, \quad (3.2)$$

where D_{hkl} is the particle size perpendicular to the normal line of (hkl) plane, k is a constant (it is 0.9), B_{hkl} is the FWHM of the (hkl) diffraction peak, θ_{hkl} is the Bragg angle of (hkl) peak and λ is the wavelength of X-rays used.

The values of the lattice parameters of the most intense diffraction peaks and the grain sizes of our annealed thin films are listed in Table 1.

Although (110) and (101) peaks are intense, (211) and (112) peaks are relatively less intense which may be explained by the reduction in the film thickness, and by the size difference between the film particles. The results indicate also a slight offset of the peak angular position which can be explained by heat treatment, stress produced during the deposit development in SnO₂

thin films and/or instrumental imperfections (including the incident wavelength). Finally, we can conclude that the thickness is an important parameter; it will have a significant role on the crystal orientation and degree of crystallinity, which improves with increasing coating repetition (cycle), i.e. with the film thickness.

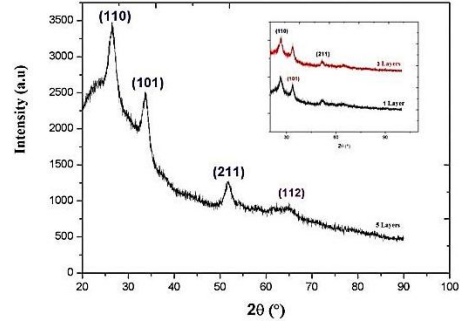


Fig. 5 – SEM X-ray diffraction patterns of SnO₂ film grown by 5 cycles (inset: diffractograms of the films: 1 cycle and 3 cycles)

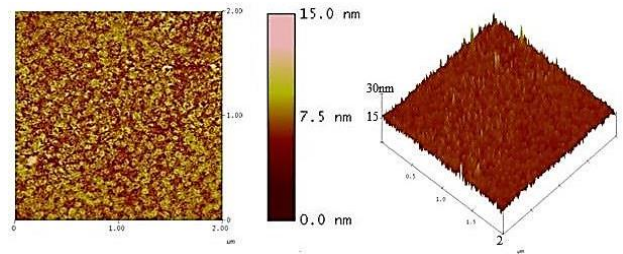


Fig. 6 – 2D and 3D AFM images of SnO₂ films grown by 5 cycles and annealed at 450 °C for 1 h in air

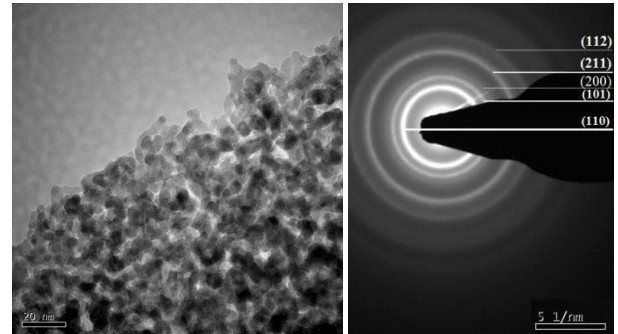


Fig. 7 – TEM images and the selected-area electron diffraction patterns of pure SnO₂ thin film elaborated by spin coating

The surface topography of SnO₂ film was studied using atomic force microscopy (AFM). Fig. 6 shows two-dimensional (2D) and 3D AFM micrographs of the same sample scanned over a surface area of $2 \times 2 \mu\text{m}^2$. The samples exhibit uniform surface where the nanoparticles grow and aggregate homogeneously and there are some white particles that grow on the film which confirm SEM observations.

In order to have more insight on the crystalline structure, the films were analyzed by TEM. Fig. 7 is a TEM bright field plane-view image of SnO₂ nanoparticles. It shows the carpet of small grains. They have a quasi-constant mean size with an average diameter of about 8 nm. It can be seen the absence of larger white grains previously observed in SEM photographs, which allows us to confirm that they have disappeared in the

Table 1 – Description of the special paragraph styles

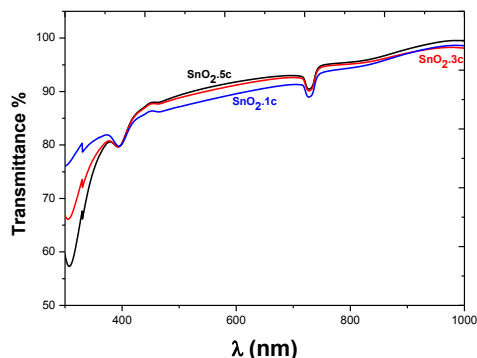
Samples	Peak pos. ($2\theta^\circ$)	Height [cts]	d_{hkl} spacing (Å)	FWHM 2θ ($^\circ$)	hkl	D_{hkl} (nm)	E_g (eV)
Sn.1 layer	26.284	77.39	3.3907	0.3124	110	26.11	–
	33.659	52.51	2.6605	0.9792	101	8.48	
Sn.3 layers	26.563	71.26	3.3557	0.3256	110	25.08	2.84
	33.834	58.56	2.6493	0.3433	101	24.20	
Sn.5 layers	26.423	1167.32	3.3732	0.4015	110	20.32	3.14
	33.908	876.95	2.6437	0.4585	101	18.11	
	51.729	263.67	1.7657	0.8160	211	10.82	

preparation of the samples to this analysis, especially during the dissolution in ethanol.

The selected-area electron diffraction (SAED) pattern displays several clear bright circular rings corresponding to various orientations, three important planes in the reciprocal space of a tetragonal structure (110), (101) and (211) in the form of continuous rings. This implies that nanoparticles have multiple orientations.

3.3 Optical Transmittance Results

The UV-Vis spectra (Fig. 8) of the films were studied using the optical transmittance measurements of SnO₂ films formed by the spin-coating method under identical spinning conditions but of different thicknesses. The elaborated films are transparent in the visible range. All films exhibit a transmission of > 85 % in the visible region. This result is similar to other reports [14, 18].

**Fig. 8** – Optical transmittance spectra of SnO₂ thin films prepared by spin-coating

As the number of layers increases, optical transmittance T (%) increases. This may be due to the improvement in the film homogeneity and its crystallinity. The microstructural and morphological characteristics depend on the thickness and crystallinity. Increased crystallinity is attributed to the improvement of stoichiometry or the reduction of the impurities or both.

It can be concluded that the transmittance of SnO₂ film increases with crystallinity improvement.

The optical band gap was evaluated from the transmission spectra. The absorption coefficient was evaluated by the transmittance T and film thickness d using Lambert law [19]:

$$\alpha = \frac{1}{d} \ln \frac{1}{T}. \quad (3.3)$$

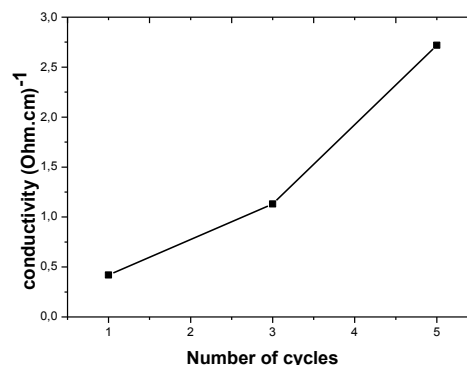
The optical absorption coefficient α near the absorption edge is given by [20]:

$$(\alpha h\nu)^2 = A(h\nu - E_g), \quad (3.4)$$

where A is a constant which is related to the effective masses associated with the bands, and E_g is the band gap energy. The direct band gap of SnO₂ thin film was estimated by plotting $(\alpha h\nu)^2$ versus the photon energy $h\nu$, and extrapolating the linear portion of the graph to the energy axis at $\alpha = 0$. The values corresponding to E_g of the produced films are listed in Table 1. It can be seen that the energy gap increases with increasing repetition of spin cycles which suggests that defects and impurities disappear when the thickness increases, which can also be correlated with the increase in grain sizes and reorganization of SnO₂ structure.

3.4 Electrical Properties

Conductivity values of SnO₂ films as can be seen in Fig. 9 are proportional to the number of layers. The conductivity of the film is found at room temperature between a minimum of $0.42 (\Omega \cdot \text{cm})^{-1}$ and a maximum of $2.72 (\Omega \cdot \text{cm})^{-1}$ (Fig. 9). The increase in conductivity can be understood in terms of the porous film morphology. The electrical conductivity is also influenced by the microstructure. It is increasing due to the improved crystallinity. SnO₂ electrical conductivity also increases due to excess Sn as an impurity (self-doping), it shows n -type conductivity.

**Fig. 9** – Variation of the electrical conductivity of SnO₂ films versus the number of layers

4. CONCLUSIONS

Transparent nanostructured tin oxide thin films were prepared onto glass substrates by spin coating with appropriate annealing conditions.

SnO₂ thin films have been studied and deposition parameters have been optimized. Thin films were characterized by a variety of techniques. The film surface is formed homogeneously of nano-sized particles with

dense microstructure confirmed by TEM images. The X-ray diffraction pattern of the crystalline SnO₂ thin films reveals the existence of single-phase rutile type tetragonal crystal structure. The increase in crystallinity with thickness is attributed to the improvement of stoichiometry or reduction of impurities or both.

The film properties are highly dependent on their structural characteristics. All the films exhibit a

transmission of > 85 % in the visible region. The electrical conductivity of the films strongly depends on crystalline structure quality.

In conclusion, varying the thickness of the tin oxide films affects its optoelectronic properties, and it may be considered that the deposited SnO₂ thin film is suitable for many optical devices, such as solar cells, gas sensors, surface acoustic devices, transparent electrodes.

REFERENCES

1. H. Liu, V. Avrutin, N. Izyumskaya, Ü. Özgür, H. Morkoç, *Superlattice. Microst.* **48**, 458 (2010).
2. T.J. Coutts, D.L. Young, X. Li, *MRS. Bull.* **25**, 58 (2000).
3. L.A. Patil, M.D. Shinde, A.R. Bari, V.V. Deo, *Sensor. Actuat. B: Chem.* **143**, 270 (2009).
4. K.L. Chopra, S. Major, D.K. Pandya, *Thin Solid Films* **102**, 1 (1983).
5. S.G. Ansari, P. Boroojerdian, S.R. Sainkar, R.N. Karekar, R.C. Aiyer, S.K. Kulkarni, *Thin Solid Films* **295**, 271 (1997).
6. R.S. Niranjana, Y.K. Hwang, D.K. Kim, S.H. Jung, S.J. Chang, I.S. Mulla, *Mater. Chem. Phys.* **92**, 384 (2005).
7. F.M. Filho, A.Z. Simoes, A. Ries, E.C. Souza, L. Perazolli, M. Cilence, E. Longo, J.A. Varela, *Ceram. Int.* **31**, 399 (2005).
8. Y. Wang, J. Ma, F. Ji, X.H. Hu, H.L. Ma, *J. Lumin.* **114**, 71 (2005).
9. W.K. Man, H. Yan, S.P. Wong, I.H. Wilson, T.K.S. Wong, *J. Vac. Sci. Technol. A* **14**, 1593 (1996).
10. T.H. Fang, W.J. Chang, *Appl. Surf. Sci.* **220**, 175 (2003).
11. B. Thangaraju, *Thin Solid Films* **402**, 71 (2002).
12. G. Zhang, M. Liu, *J. Mat. Sci.* **34**, 3213 (1999).
13. Z. Chen, J.K.L. Lai, C.H. Shek, H. Chen, *J. Mater. Res.* **18**, 1289 (2003).
14. M.M. Bagheri-Mohagheghi, M. Shokoh-Saremi, *J. Phys. D: Appl. Phys.* **37**, 1248 (2004).
15. M. Maache, T. Devers, A. Chala, *Semiconductors* **51**, 1604 (2017).
16. Y.C. Goswami, V. Kumar, V. Ganesan, P. Rajaram, *AIP Conf. Proc.* **1512**, 1290 (2013).
17. C.S. Barrett, T.B. Massalski, *Structure of Metals* (Oxford: Pergamon Press: 1980).
18. M.M. Bagheri-Mohagheghi, N. Shahtahmasebi, M.R. Alinejad, A. Youssefi, M. Shokoh-Saremi, *Physica B* **403**, 2431 (2008).
19. D. Bao, X. Wu, L. Zhang, X. Yao, *Thin Solid Films* **350**, 30 (1999).
20. D.R. Sahu, *Microelectron. J.* **38**, 1252 (2007).

Характеристики тонких плівок оксиду олова, отриманих методом центрифугування, для оптоелектронних застосувань

М. Мааче^{1,2}, А. Чала^{2,3}, Т. Деверс⁴

¹ Department of Physics, Ziane ACHOUR University, 17000 Djelfa, Algeria

² PLTFA, Physical laboratory of thin films and applications, Mohamed KHIDER University, 07000 Biskra, Algeria

³ Department of Science of matter, Mohamed KHIDER University, 07000 Biskra, Algeria

⁴ University of Orléans, ICMN-UMR 7374 CNRS, IUT of Chartres, 28000 Chartres, France

Золь-гелеву техніку застосовували для отримання тонких плівок чистого оксиду олова (SnO₂). Плівки вирощували при кімнатній температурі на чистих скляних підкладках методом центрифугування. Дигідрат хлористого олова (II) використовували як вихідний матеріал, а 2-пропанол – як розчинник. Молярність олова зберігалася [Sn²⁺] = 0.3 М. На мікрофотографіях SEM опрацьованих плівок видно, що вони складаються із дуже дрібнозернистих частинок. XRD аналіз виявляє, що всі відпалені плівки складаються з однофазного SnO₂, дифрактограми вказують на наявність піків (100), (101), (211), що відповідають тетрагональній фазі без будь-яких вторинних фаз. Зображення скануючої електронної мікроскопії та атомно-силової мікроскопії показують еволюцію різних поверхневих морфологій; усі плівки мають однорідну та рівномірну морфологію поверхні. Просвічуюча електронна мікроскопія підтверджує, що підготовлені плівки є нанокристалічними. Крім того, досліджується вплив багат шарового покриття на оптоелектронні властивості тонких плівок SnO₂. У видимій області пропускна здатність перевищує 85 %. Питомий опір тонких плівок SnO₂ значно зменшується з товщиною. Орієнтовне максимальне значення провідності становить 2.72 (Ω.см)⁻¹.

Ключові слова: SnO₂, Золь-гель, Спінове покриття, Провідність, Оптоелектронний.